LAWRENCE
LIVERMORE
NATIONAL
LABORATORY

LLNL-JRNL-414669

Spectroscopy of M-shell x-ray transitions in Zn-like through Co-like W

J. Clementson, P. Beiersdorfer, G. V. Brown, M. F. Gu

July 13, 2009

Physica Scripta

Disclaimer

Spectroscopy of M-shell x-ray transitions in Zn-like through Co-like W

J Clementson*, P Beiersdorfer, G V Brown and M F Gu§

Lawrence Livermore National Laboratory, Livermore, CA 94550, USA

E-mail: clementson@llnl.gov

Abstract. The M-shell x-ray emission of highly charged tungsten ions has been investigated at the Livermore electron beam ion trap facility. Using the SuperEBIT electron beam ion trap and a NASA x-ray calorimeter array, transitions connecting the ground configurations in the 1500 - 3600 eV spectral range of zinc-like W^{44+} through cobalt-like W^{47+} have been measured. The measured spectra are compared with theoretical line positions and emissivities calculated using the FAC code.

1. Introduction

Tungsten is gaining interest in fusion engineering as a plasma facing material in magnetic confinement devices, see e.g. [1, 2, 3]. Some present day tokamaks are already operating with tungsten surfaces or are currently installing tungsten parts [4]. The ITER tokamak, now under construction in Cadarache, France, will have a tungsten divertor.

The use of tungsten in magnetic fusion experiments will introduce trace amounts of tungsten ions into the high-temperature low-density plasmas. Tungsten ions that enter into a tokamak will not become fully stripped even in the hot core, resulting in strong x-ray emission over a wide range of temperatures. Provided the spectra are well understood, the tungsten ions can serve as diagnostics for plasma parameters [5, 6]. For instance, the ion temperatures of the ITER core plasmas will likely be measured using the Doppler broadening of L-shell tungsten lines.

Forty-six times ionized nickel-like tungsten has twenty-eight electrons arranged in a filled M-shell structure (unlike Ni I with a ground configuration of $3s^2 3p^6 3d^4_{3/2} 3d^4_{5/2} 4s^2$) and is therefore abundant over a large temperature range in high-temperature plasmas. This makes the nickel-like tungsten spectrum important for diagnostic purposes. The tungsten M-shell spectra of nickel-like and neighboring charge states have been extensively investigated, see for example Refs. [5, 7, 8, 9, 10, 11, 12, 13, 14, 15, 16, 17, 18, 19, 20, 21, 22, 23, 24, 25, 26, 27, 28]. Further references can be found in the Kramida and Shirai review of atomic data for tungsten ions [29].

* Also at Department of Physics, Lund University, P. O. Box 118, SE-221 00 Lund, Sweden

§ Present address at Space Sciences Laboratory, University of California, Berkeley, CA 94720, USA

In recent years Neill et al. [12], Safronova et al. [15, 16], and Ralchenko et al. [19] have measured M-shell tungsten spectra on electron beam ion traps: the Livermore EBIT-II, the Livermore EBIT-I and EBIT-II, and the NIST EBIT, respectively. Safronova et al. and Ralchenko et al. used x-ray calorimeter spectrometers for broadband spectral surveys. X-ray calorimeters (also known as quantum calorimeters or microcalorimeters) offer lower spectroscopic resolution than crystal spectrometers, however the higher throughput and the very broad spectral coverage make these novel spectrometers very useful for the study of atomic spectra. Especially measurements of high-Z ions that have several transition bands benefit from x-ray calorimeters. For instance, recently high charge states of Au were observed at the Livermore SuperEBIT, enabling line identifications and charge balance modeling [30]. In this paper, we report on the application of an x-ray calorimeter array at SuperEBIT to derive spectral line positions of M-shell x-ray transitions of W^{44+} through W^{47+}.

2. Experimental setup

The measurements were carried out using the SuperEBIT electron beam ion trap at the Lawrence Livermore National Laboratory. SuperEBIT was operated in a low-energy configuration, making it similar to EBIT-I [31], at beam energies close to 3.3 keV, 4.0 keV, and 4.1 keV. These energies are of interest for the study of nickel-like tungsten which is created from copper-like tungsten at 2414.1 eV and ionizes to cobalt-like at 4057 eV [32].

The tungsten ions were injected into the SuperEBIT trap using one of two methods: Metal Vapor Vacuum Arc (MeVVA) injection and sublimation injection. Most of the data were acquired using the faster sublimation injection. For this method, sublimation of tungsten hexacarbonyl, $W(CO)_6$, occurred in a vial attached to one of SuperEBIT's six radial vacuum ports. Once in gaseuous form, $W(CO)_6$ molecules freely entered the trap region through the port. As tungsten carbonyl molecules continuously fill the trap, the charge state distributions typically consist of several tungsten ions. The MeVVA injector discharges bunches of low charge state ions into the trap from a tungsten cathode, located at the top of SuperEBIT, once every trap cycle. As a result, the EBIT plasmas have a more peaked charge state distribution. Sodium metal was also sublimated and injected as neutral gas, which, together with low-Z plasma impurities, provided reference spectra for energy calibration.

The x-ray emission was recorded with a NASA X-Ray Spectrometer (XRS) x-ray calorimeter [33, 34, 35] designed at the Goddard Space Flight Center. The XRS spectrometer is a medium-resolution energy-dispersive instrument for soft and hard x-rays made up of an array of HgTe and Bi heat absorbers. For this measurement 23 of the HgTe pixel elements were used, providing a resolution of 6.5 eV full width at half maximum, which, for the interval of interest, equals a resolving power $E/\Delta E = 230$ - 550. The data from the elements used for the measurement were corrected for voltage drifts and added together.

3. Calculations and Spectral Modeling

The transition energies of zinc-like through cobalt-like tungsten were calculated using the fully relativistic atomic physics package FAC v1.1.1 [36]. Keeping the K- and L-shells closed, energy levels and transition energies were calculated for the M- and N-shells. Table 1 lists included configuration state functions.

Collisional-radiative models were constructed for the spectra of the four tungsten ions. The plasmas were modeled with electron beam energies of 3.3 keV and 4.1 keV at an electron density of 5×10^{11} cm^{-3}. Electron impact excitation and deexcitation were included as well as autoionization for the Cu- and Zn-like charge states. The calculated spectra for an excitation energy of 4.1 keV and line widths of 6.5 eV are shown in Fig. 1.

4. Experimental Tungsten Spectra

Analyzed spectra include tungsten hexacarbonyl data obtained at beam energies close to 3.3, 4.0, and 4.1 keV, and MeVVA data obtained at a beam energy of 4.1 keV. The 4.1 keV carbonyl spectrum was energy calibrated with the $3s^23p^63d^{10}$ — $(3s^23p^63d^3_{3/2}3d^6_{5/2}4p_{1/2})_1$ Ni-like W line, which has been accurately measured at EBIT-I by Elliott et al. [26], and with K-shell emission from low-Z elements (Na, Si, Cl, Ar, and K) with transition energies calculated by Garcia and Mack [37], Drake [38], and Vainshtein and Safronova [39]. Ni-like W line positions determined from this spectrum were then used as reference lines in the other spectra. Conversion factors used were $hc = 12398.42$ Å·eV $= 8065.5410$ eV·cm.

The broadband XRS spectra are dominated by Ni-like W lines with upper levels from $n = 4$, 5, 6, 7, and 8. Lines from the lower charge states are often blended. The measured energies of the Co-like lines are from the 4.1 keV MeVVA spectrum, and the Cu- and Zn-like line positions are derived from 3.3 keV and 4.0 keV spectra. The position of a given line, which was measured more then once, was averaged. An overview spectrum covering the 1 - 4 keV spectral band at a beam energy of 4.0 keV is shown in Fig. 2. The 3.3 keV spectrum, divided into three energy regions, is shown in Fig. 3, and the 4.1 keV spectrum, also divided, is shown in Fig. 4. The high-n transitions in Ni-like W are measured in the 4.1 keV spectrum and are shown in Fig. 5. This spectrum also shows lines from impurity ions.

The measured lines are listed in Tables 2 - 5 together with the theoretical line positions calculated with FAC. Most measured features have very good counting statistics and the spectroscopic accuracy is limited by the calibration uncertainty, which varies from 0.3 to 0.5 eV. The total uncertainty of the line positions consists of the errors associated with the counting statistics and the energy scale added in quadrature. Only features that are dominated by transitions from one charge state are listed, and some features that are too broad or not fully resolved have been omitted. For the somewhat weaker or broader features the error bars have been doubled. The XRS is energy dispersive and measures photon energies, but corresponding wavelengths are also

listed in the tables.

In the following we discuss the results obtained for each of the four charge states of tungsten we have investigated.

4.1. Zn-like W $^{44+}$

The Zn-like lines are the weakest of the four charge states investigated. Seven lines are identified and listed in Table 2. Line Zn-3 and one of the Zn-4 transitions are 2-electron 1-photon decays. Neill et al. [12] observed these lines and assigned Zn-3 to be a Ga-like W line and Zn-4 to be a resonance line emanating from the $3d^3_{3/2}3d^6_{5/2}4s^24f_{5/2}$ configuration. As pointed out by Kramida and Shirai [29], the two lines should be 2-electron 1-photon decays to the ground state. Kramida and Shirai suggest the lines to be from $3d^3_{3/2}3d^6_{5/2}4s_{1/2}4p_{3/2}4d_{3/2}$. Here, the FAC kinetic model suggests one of those lines instead to be from $3d^3_{3/2}3d^6_{5/2}4s_{1/2}4p_{3/2}4d_{5/2}$. The calculations also suggest the Zn-4 line to be blended with two 2-electron 1-photon resonance decays in Cu-like W (from upper level $(3s^23p^63d^3_{3/2}3d^6_{5/2}4p_{3/2}4d_{3/2})_{3/2}$ at 2155.2 and 2158.3 eV). Zn-3 possibly blends with two Ga-like transitions ($3d^{10}4s^24p_{1/2}$ - $3d^3_{3/2}3d^6_{5/2}4s^24p_{1/2}4f_{5/2}$), and Zn-5 possibly blends with a Ge-like line ($3d^{10}4s^24p^2_{1/2}$ - $3d^3_{3/2}3d^6_{5/2}4s^24p^2_{1/2}5f_{5/2}$). The error bars of the energies associated with Zn-3, Zn-4, and Zn-5 have therefore been doubled.

4.2. Cu-like W $^{45+}$

Ten Cu-like features are reported in Table 3. The lines are measured in the 3.3 keV and 4.0 keV spectra. Cu-8 is possibly blended with a Ga-like resonance transition (emanating from the $3d^3_{3/2}3d^6_{5/2}4p_{1/2}5f_{5/2}$ configuration), and hence, the error bar has been doubled.

4.3. Ni-like W $^{46+}$

Twenty-seven nickel-like tungsten lines are identified and listed in Table 4. They were mostly measured in the 4.1 keV spectrum, although many are average line positions from several spectra. Ni-1 and Ni-2 are weak N-shell transitions, whereas the other observed lines are M-shell transitions. Ni-3 is made up of two energetically close dipole forbidden transitions (cf. [40]); a magnetic octupole and an electric quadrupole transition. These lines have recently been resolved with high-resolution crystal spectrometers [41]. The Ni-10 line position has been predicted by [10, 29] but has not previously been observed (here it is one of the weakest lines). A previously doubly classified line observed by Tragin et al. [24] (also discussed in [29]), is resolved in this work, Ni-23 and Ni-24. As noted by Kramida and Shirai [29], the previously doubly classified line Ni-26 [24] should be dominated by one transition.

4.4. Co-like W $^{47+}$

The features from cobalt-like tungsten were all measured in the 4.1 keV MeVVA spectrum and are listed in Table 5. Co-like W has many transitions and only the

dominating transitions in each feature are tabulated. The error bars for some of the weaker features have been doubled. Co-4 blends with two transitions at slightly lower energy giving the line a shoulder.

According to our FAC calculations, previous identifications for Co-12 [12, 29] are not correct. The 2227.4 eV transition is misidentified in [12] and the identifications for the 2227.4 eV and the 2230.9 eV transitions seem to be interchanged in [29]. The coupling for the 2145.9 eV transition in Co-10 also seems incorrect in [29].

5. Summary

The M-shell spectra of Zn-like through Co-like W ions have been measured using an x-ray calorimeter spectrometer at the SuperEBIT electron beam ion trap. Spectra were studied at excitation energies 3.3 keV, 4.0 keV, and 4.1 keV and show strong line emission in the 1500 - 3600 eV soft x-ray range. Line positions determined in our measurement are generally in good agreement with previous measurements when available and have significantly higher accuracies. Some of our lines have similar positions and error bars as those found earlier, but have been assigned to different transitions. This is likely to be due to the higher electron densities of the earlier experiments. A few lines, however, disagree with the work of Neill et al. [12], although their measurements were performed at similar densities as ours. In addition, many lines have been presented which have been identified for the first time

Relativistic atomic structure and collisional-radiative calculations have been performed using the FAC atomic physics code. Theoretical spectra are presented for Zn-like W^{44+} through Co-like W^{47+}. Very good agreement is established between calculated and observed spectra.

Acknowledgments

This work was performed under the auspices of the United States Department of Energy by Lawrence Livermore National Laboratory under contract DE-AC52-07NA-27344. The authors would like to acknowledge assistance with the experiment from Phil D'Antonio, Ed Magee, Dr. Daniel Thorn, and Prof. Elmar Träbert. Joel Clementson would like to thank Dr. Hans Lundberg, Dr. Sven Huldt, and Prof. Sune Svanberg for their support.

References

[1] Peacock N J, O'Mullane M G, Barnsley R and Tarbutt M 2008 *Can. J. Phys.* **86** 277–284
[2] Skinner C H 2008 *Can. J. Phys.* **86** 285–290
[3] Skinner C H 2009 *Phys. Scr.* **T134** 014022
[4] Neu R, Dux R, Kallenbach A, Pütterich T, Balden M, Fuchs J C, Herrmann A, Maggi C F, O'Mullane M, Pugno R, Radivojevic I, Rohde V, Sips A C C, Suttrop W, Whiteford A and the ASDEX Upgrade team 2005 *Nucl. Fusion* **45** 209–218
[5] Biedermann C, Radtke R, Seidel R and Pütterich T 2009 *Phys. Scr.* **T134** 014026

[6] Reader J 2009 *Phys. Scr.* **T134** 014023
[7] Dong C Z, Fritzsche S and Xie L Y 2003 *J. Quant. Spectrosc. Radiat. Transfer* **76** 447–465
[8] Aggarwal K M, Norrington P H, Bell K L, Keenan F P, Pert G J and Rose S J 2000 *At. Data Nucl. Data Tables* **74** 157–255
[9] Fournier K B 1998 *At. Data Nucl. Data Tables* **68** 1–48
[10] Zigler A, Zmora H, Spector N, Klapisch M, Schwob J L and Bar-Shalom A 1980 *J. Opt. Soc. Am.* **70** 129–132
[11] Zigler A, Klapisch M and Mandelbaum P 1986 *Phys. Lett. A* **117** 31–35
[12] Neill P, Harris C, Safronova A S, Hamasha S, Hansen S, Safronova U I and Beiersdorfer P 2004 *Can. J. Phys.* **82** 931–942
[13] Neu R, Fournier K B, Schlögl D and Rice J 1997 *J. Phys. B: At. Mol. Opt. Phys.* **30** 5057–5067
[14] Neu R, Fournier K B, Bolshukhin D and Dux R 2001 *Phys. Scr.* **T92** 307–310
[15] Safronova A S, Kantsyrev V L, Neill P, Safronova U I, Fedin D A, Ouart N D, Yilmaz M F, Osborne G, Shrestha I, Williamson K, Hoppe T, Harris C, Beiersdorfer P and Hansen S 2008 *Can. J. Phys.* **86** 267–276
[16] Shlyaptseva A, Fedin D, Hamasha S, Harris C, Kantsyrev V, Neill P, Ouart N and Safronova U 2004 *Rev. Sci. Instrum.* **75** 3750–3752
[17] Osborne G C, Safronova A S, Kantsyrev V L, Safronova U I, Yilmaz M F, Williamson K M, Shrestha I and Beiersdorfer P 2008 *Rev. Sci. Instrum.* **79** 10E308
[18] Loch S D, Pindzola M S, Ballance C P, Griffin C P, Whiteford A D and Pütterich T 2006 *Spectral Line Shapes: 18th International Conference* ed Oks E and Pindzola M (American Institute of Physics)
[19] Ralchenko Y, Tan J N, Gillasy J D, Pomeroy J M and Silver E 2006 *Phys. Rev. A* **74**
[20] Ralchenko Y 2007 *J. Phys. B: At. Mol. Opt. Phys.* **40**
[21] Hamasha S M, Shlyaptseva A S and Safronova U I 2004 *Can. J. Phys.* **82** 331–356
[22] Klapisch M, Mandelbaum P, Barshalom A, Schwob J L, Zigler A and Jackel S 1981 *J. Opt. Soc. Am.* **71** 1276–1281
[23] Mandelbaum P, Klapisch M, Bar-Shalom A, Schwob J L and Zigler A 1983 *Phys. Scr.* **27** 39–53
[24] Tragin N, Geindre J P, Monier P and Gauthier J C 1988 *Phys. Scr.* **37** 72–82
[25] Burkhalter P G, Dozier C M and Nagel D J 1977 *Phys. Rev. A* **15** 700–717
[26] Elliott S R, Beiersdorfer P, MacGowan B J and Nilsen J 1995 *Phys. Rev. A* **52** 2689–2692
[27] Pütterich T, Neu R, Dux R, Whiteford A D, O'Mullane M G and the ASDEX Upgrade Team 2008 *Plasma Phys. Control. Fusion* **50** 1–27
[28] Ballance C P and Griffin D C 2006 *J. Phys. B: At. Mol. Opt. Phys.* **39** 3617–3628
[29] Kramida A E and Shirai T 2009 *At. Data Nucl. Data Tables* **95** 305–474
[30] Brown G V, Hansen S B, Träbert E, Beiersdorfer P, Widmann K, Chen H, Chung H K, Clementson J H T, Gu M F and Thorn D B 2008 *Phys. Rev. E* **77** 066406
[31] Levine M A, Marrs R E, Henderson J R and Knapp D A Schneider M B 1988 *Phys. Scr.* **T22** 157–163
[32] Kramida A E and Reader J 2006 *At. Data Nucl. Data Tables* **92** 457–479
[33] Porter F S, Brown G V, Boyce K R, Kelley R L, Kilbourne C A, Beiersdorfer P, Chen H, Terracol S, Kahn S M and Szymkowiak A E 2004 *Rev. Sci. Instrum.* **75** 3772–3774
[34] Brown G V, Beiersdorfer P, Boyce K R, Chen H, Gu M F, Kahn S M, Kelley R L, Kilbourne C A, May M, Porter F S, Szymkowiak A E, Thorn D and Widmann K 2006 *Nucl. Instrum. Methods Phys. Res., Sect. A* **559** 623–625
[35] Porter F S, Beck B R, Beiersdorfer P, Boyce K R, Brown G V, Chen H, Gygax J, Kahn S M, Kelley R L, Kilbourne C A, Magee E and Thorn D B 2008 *Can. J. Phys.* **86** 231–240
[36] Gu M F 2008 *Can. J. Phys.* **86** 675–689
[37] Garcia J D and Mack J E 1965 *J. Opt. Soc. Am.* **55** 654–685
[38] Drake G W 1988 *Can. J. Phys.* **66** 586–611
[39] Vainshtein L A and Safronova U I 1985 *Phys. Scr.* **31** 519–532

[40] Beiersdorfer P, Osterheld A L, Scofield J, Wargelin B and Marrs R E 1991 *Phys. Rev. Lett.* **67** 2272–2275
[41] Clementson J, Beiersdorfer P and Gu M F 2009 In preparation
[42] Butzbach R, Daido H, Förster E, Gu Y, Huang G, Kato Y, Koike F, Sebban S, Tang H, Uschmann I, Vollbrecht M and Wang S 1999 *Papers presented at x-ray lasers conf, Kyoto, Japan, August 31 - September 4, 1998* 159 (Institute of Physics) p 463
[43] Wyart J F, Bauche-Arnoult C, Gauthier J C, Geindre J P, Monier P, Klapisch M, Bar-Shalom A and Cohn A 1986 *Phys. Rev. A* **34** 701

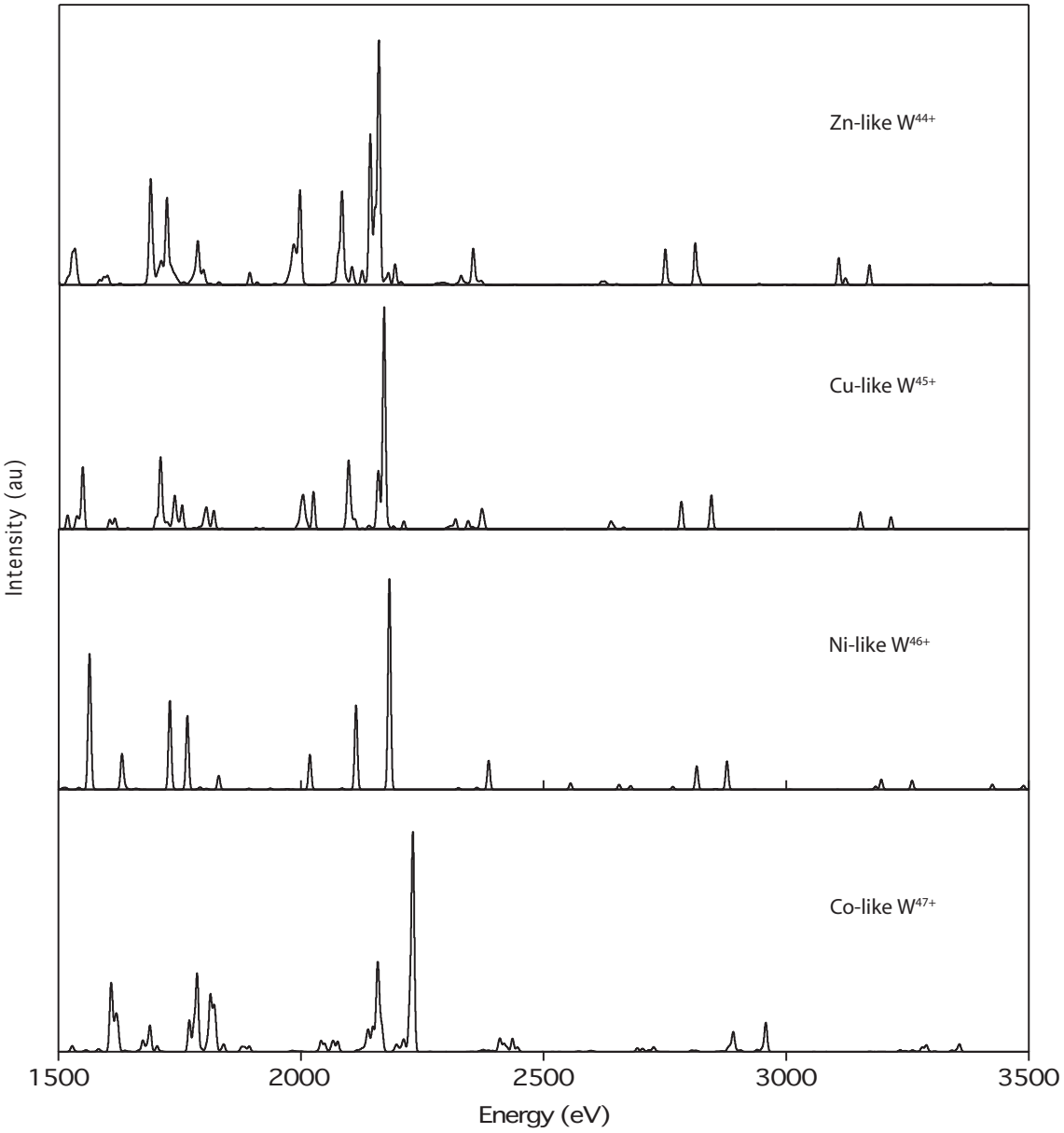

Figure 1. Calculated tungsten spectra at an excitation energy 4.1 keV. The assumed line width is 6.5 eV.

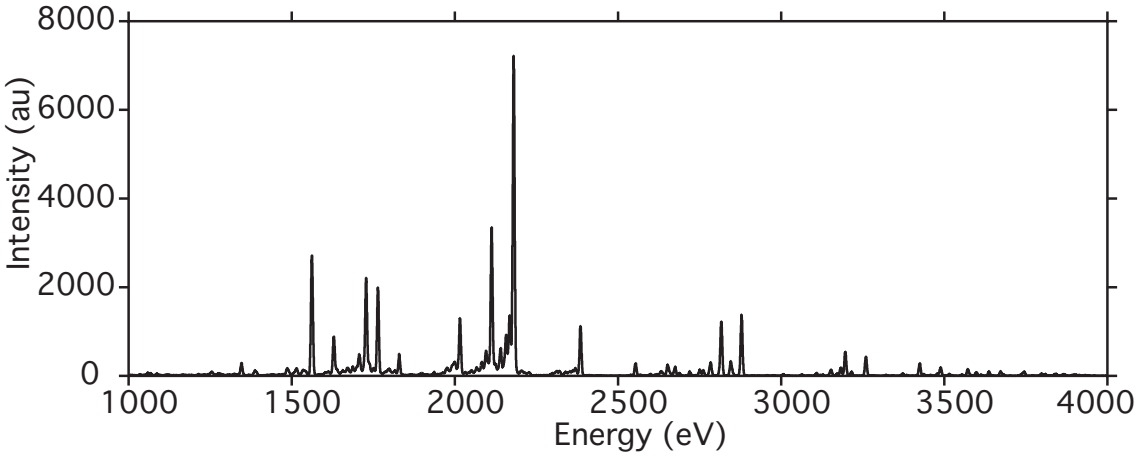

Figure 2. SuperEBIT XRS spectrum recorded at an electron beam energy of 4.0 keV.

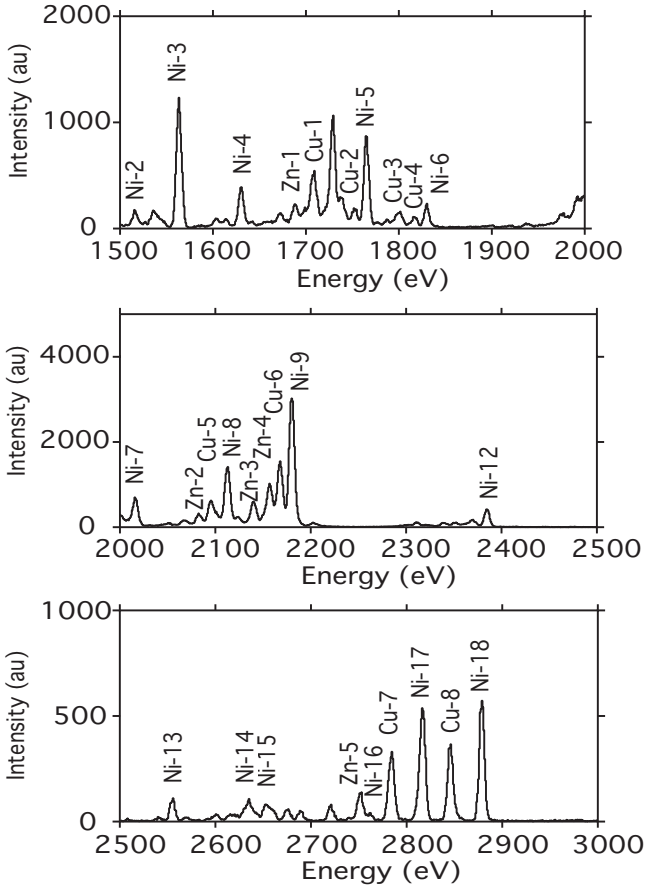

Figure 3. SuperEBIT XRS spectra recorded at an electron beam energy of 3.3 keV.

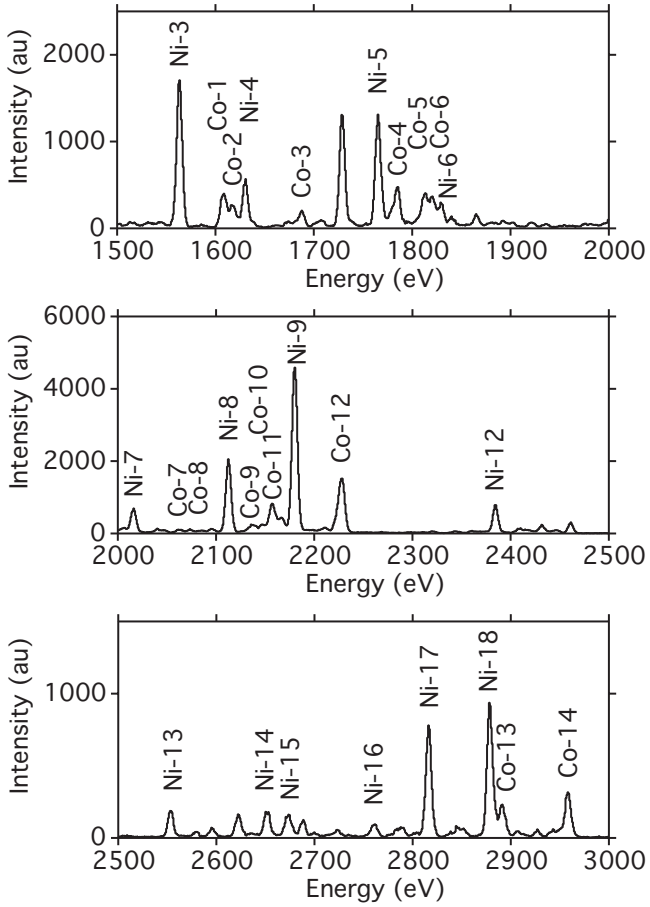

Figure 4. SuperEBIT XRS spectra recorded at an electron beam energy of 4.1 keV.

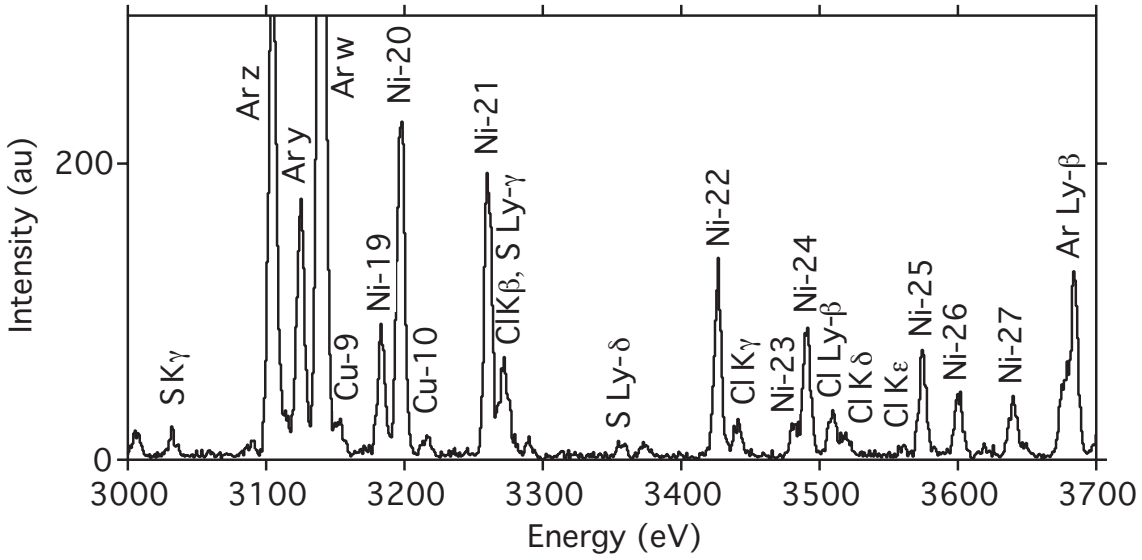

Figure 5. High-n transitions of Ni-like W^{46+} recorded at an electron beam energy of 4.1 keV.

Zn	Cu	Ni	Co
$3s^23p^63d^{10}4lnl$	$3s^23p^63d^{10}nl$	$3s^23p^63d^{10}$	$3s^23p^63d^9$
			$3s^23p^53d^{10}$
			$3s3p^63d^{10}$
$3s^23p^63d^94l4l4l$	$3s^23p^63d^94l4l$	$3s^23p^63d^9nl$	$3s^23p^63d^8nl$
$3s^23p^63d^94l^*4l^*nl$	$3s^23p^63d^94l^*nl$		$3s^23p^53d^9nl$
			$3s3p^63d^9nl$
$3s^23p^53d^{10}4l4l4l$	$3s^23p^53d^{10}4l4l$	$3s^23p^53d^{10}nl$	$3s^23p^53d^9nl$
$3s^23p^53d^{10}4l^*4l^*nl$	$3s^23p^53d^{10}4l^*nl$		$3s^23p^43d^{10}nl$
			$3s3p^53d^{10}nl$
$3s3p^63d^{10}4l4l4l$	$3s3p^63d^{10}4l4l$	$3s3p^63d^{10}nl$	$3s3p^63d^9nl$
$3s3p^63d^{10}4l^*4l^*nl$	$3s3p^63d^{10}4l^*nl$		$3s3p^53d^{10}nl$
			$3p^63d^{10}nl$

Table 1. Configuration state functions included in the structure calculations with n = 5, 6 for Zn and Cu, n = 4 - 8 for Ni, and n = 4, 5, 6 for Co. l = 0, 1, ..., n - 1. l^* = s, p.

Key	Transition		Theory	Experiment		Prev. Exp.
	lower level	upper level	ΔE (eV)	ΔE (eV)	λ (Å)	λ (Å)
Zn-1	$3s^23p^63d^{10}4s^2$	$(3s^23p^63d^3_{3/2}3d^6_{5/2}4s^24p_{1/2})_1$	1688.1	1688.4(8)	7.3433(35)	$7.332(3)^{M*1}$
						7.34^{Ne}
Zn-2	$3s^23p^63d^{10}4s^2$	$(3s^23p^63d^4_{3/2}3d^5_{5/2}4s^24f_{7/2})_1$	2082.6	2082.2(4)	5.9545(11)	
Zn-3	$3s^23p^63d^{10}4s^2$	$(3s^23p^63d^3_{3/2}3d^6_{5/2}4s_{1/2}4p_{3/2}4d_{3/2})_1$	2141.3	2139.7(8)	5.7945(22)	5.7928^{N*2}
Zn-4	$3s^23p^63d^{10}4s^2$	$(3s^23p^63d^3_{3/2}3d^6_{5/2}4s_{1/2}4p_{3/2}4d_{5/2})_1$	2150.6	2156.4(16)	5.7496(42)	5.7676^{N*3}
	$3s^23p^63d^{10}4s^2$	$(3s^23p^63d^3_{3/2}3d^6_{5/2}4s^24f_{5/2})_1$	2159.0			5.7471^{N*4}
Zn-5	$3s^23p^63d^{10}4s^2$	$(3s^23p^63d^4_{3/2}3d^5_{5/2}4s^25f_{7/2})_1$	2750.2	2750.3(10)	4.5080(16)	$4.507(2)^{T*5}$
						4.509^{Z1*5}
Zn-6	$3s^23p^63d^{10}4s^2$	$(3s^23p^63d^4_{3/2}3d^5_{5/2}4s^26f_{7/2})_1$	3107.9	3107.8(5)	3.9895(6)	$3.990(5)^{T}$
						3.988^{Z1}
Zn-7	$3s^23p^63d^{10}4s^2$	$(3s^23p^63d^3_{3/2}3d^6_{5/2}4s^26f_{5/2})_1$	3171.0	3171.2(6)	3.9097(7)	$3.909(5)^{T}$
						3.909^{Z1}

Table 2. Zn-like W^{44+} line positions measured with the NASA XRS spectrometer. Theoretical energies are from the present FAC calculations. ^{M} Mandelbaum et al. [23], ^{N} Neill et al. [12], ^{Ne} Neu et al. [13], ^{T} Tragin et al. [24], ^{Z1} Zigler et al. [11]. Superscripts *xx denote comments on previous measurement found in Table 6.

Key	Transition lower level	upper level	Theory ΔE (eV)	Experiment ΔE (eV)	λ (Å)	Prev. Exp. λ (Å)
Cu-1	$3s^23p^63d^{10}4s_{1/2}$	$(3s^23p^63d^3_{3/2}3d^6_{5/2}4s_{1/2}4p_{1/2})_{3/2}$	1707.3	1707.4(6)	7.2616(26)	$7.262(3)^{M}$
						7.26^{Ne}
		$(3s^23p^63d^3_{3/2}3d^6_{5/2}4s_{1/2}4p_{1/2})_{1/2}$	1708.4			$7.262(3)^{M}$
						7.26^{Ne}
Cu-2	$3s^23p^63d^{10}4s_{1/2}$	$(3s^23p^63d^4_{3/2}3d^5_{5/2}4s_{1/2}4p_{3/2})_{3/2}$	1752.6	1751.9(8)	7.0771(32)	$7.075(3)^{M*6}$
Cu-3	$3s^23p^63d^{10}4s_{1/2}$	$(3s^23p^63d^3_{3/2}3d^6_{5/2}4s_{1/2}4p_{3/2})_{1/2}$	1797.6	1799.7(8)	6.8892(31)	$6.896(3)^{M}$
		$(3s^23p^63d^3_{3/2}3d^6_{5/2}4s_{1/2}4p_{3/2})_{3/2}$	1801.4			$6.884(3)^{M}$
	$3s^23p^63d^{10}4p_{3/2}$	$(3s^23p^63d^3_{3/2}3d^6_{5/2}4s_{1/2}4d_{3/2})_{1/2}$	1803.8			
Cu-4	$3s^23p^63d^{10}4s_{1/2}$	$(3s^23p^63d^3_{3/2}3d^6_{5/2}4s_{1/2}4p_{3/2})_{1/2}$	1817.2	1816.6(10)	6.8251(38)	$6.827(3)^{M}$
	$3s^23p^63d^{10}4p_{3/2}$	$(3s^23p^63d^3_{3/2}3d^6_{5/2}4p^2_{3/2})_{1/2}$	1818.4			$6.816(3)^{M*7}$
Cu-5	$3s^23p^63d^{10}4s_{1/2}$	$(3s^23p^63d^4_{3/2}3d^5_{5/2}4s_{1/2}4f_{7/2})_{3/2}$	2094.9	2094.8(5)	5.9187(14)	5.9127^{N*8}
		$(3s^23p^63d^4_{3/2}3d^5_{5/2}4s_{1/2}4f_{7/2})_{1/2}$	2097.7			5.9127^{N*8}
Cu-6	$3s^23p^63d^{10}4s_{1/2}$	$(3s^23p^63d^4_{3/2}3d^6_{5/2}4s_{1/2}4f_{5/2})_{1/2}$	2168.6	2167.5(4)	5.7201(11)	5.7240^{N*9}
		$(3s^23p^63d^3_{3/2}3d^6_{5/2}4s_{1/2}4f_{5/2})_{3/2}$	2169.8			5.7191^{N*10}
Cu-7	$3s^23p^63d^{10}4s_{1/2}$	$(3s^23p^63d^4_{3/2}3d^5_{5/2}4s_{1/2}5f_{7/2})_{1/2}$	2780.5	2783.0(8)	4.4551(13)	$4.457(5)^{T*11}$
		$(3s^23p^63d^4_{3/2}3d^5_{5/2}4s_{1/2}5f_{7/2})_{3/2}$	2783.1			$4.457(5)^{T*11}$
						4.458^{Z1*11}
Cu-8	$3s^23p^63d^{10}4s_{1/2}$	$(3s^23p^63d^3_{3/2}3d^6_{5/2}4s_{1/2}5f_{5/2})_{1/2}$	2843.4	2845.1(4)	4.3578(6)	$4.359(5)^{T}$
		$(3s^23p^63d^3_{3/2}3d^6_{5/2}4s_{1/2}5f_{5/2})_{3/2}$	2844.7			$4.359(5)^{T}$
						4.358^{Z1}
Cu-9	$3s^23p^63d^{10}4s_{1/2}$	$(3s^23p^63d^4_{3/2}3d^5_{5/2}4s_{1/2}6f_{7/2})_{1/2}$	3150.7	3152.5(5)	3.9329(6)	$3.933(2)^{T*12}$
		$(3s^23p^63d^4_{3/2}3d^5_{5/2}4s_{1/2}6f_{7/2})_{3/2}$	3151.9			$3.933(2)^{T*12}$
						3.932^{Z1}
Cu-10	$3s^23p^63d^{10}4s_{1/2}$	$(3s^23p^63d^3_{3/2}3d^6_{5/2}4s_{1/2}6f_{5/2})_{3/2}$	3214.7	3215.8(5)	3.8555(6)	$3.856(5)^{T}$
		$(3s^23p^63d^3_{3/2}3d^6_{5/2}4s_{1/2}6f_{5/2})_{1/2}$	3215.0			$3.856(5)^{T}$

Table 3. Cu-like W^{45+} line positions measured with the NASA XRS spectrometer. Theoretical energies are from the present FAC calculations. ^{M} Mandelbaum et al. [23], ^{N} Neill et al. [12], ^{Ne} Neu et al. [13], ^{T} Tragin et al. [24], ^{Z1} Zigler et al. [11]. Superscripts *xx denote comments on previous measurement found in Table 6.

Key	Transition lower level	upper level	Theory ΔE (eV)	Experiment ΔE (eV)	λ (Å)	Prev. Exp. λ (Å)
Ni-1	$(3s^2 3p^6 3d^3_{3/2} 3d^6_{5/2} 4p_{1/2})_1$	$(3s^2 3p^6 3d^3_{3/2} 3d^6_{5/2} 6d_{3/2})_0$	1487.0	1488.2(4)	8.3312(22)	$8.326(11)^R$
Ni-2	$(3s^2 3p_{1/2} 3p^4_{3/2} 3d^{10} 4s_{1/2})_1$	$(3s^2 3p_{1/2} 3p^4_{3/2} 3d^{10} 6p_{1/2})_0$	1515.9	1515.2(6)	8.1827(32)	
Ni-3	$3s^2 3p^6 3d^{10}$	$(3s^2 3p^6 3d^4_{3/2} 3d^5_{5/2} 4s_{1/2})_3$	1562.1	1562.9(3)	7.9330(15)	$7.930(5)^R$
		$(3s^2 3p^6 3d^4_{3/2} 3d^5_{5/2} 4s_{1/2})_2$	1564.1			$7.930(5)^R$
						7.93^{Ne}
Ni-4	$3s^2 3p^6 3d^{10}$	$(3s^2 3p^6 3d^3_{3/2} 3d^6_{5/2} 4s_{1/2})_2$	1630.0	1629.8(3)	7.6073(14)	$7.607(6)^R$
Ni-5	$3s^2 3p^6 3d^{10}$	$(3s^2 3p^6 3d^4_{3/2} 3d^5_{5/2} 4p_{3/2})_1$	1764.8	1764.6(3)	7.0262(12)	$7.028(3)^M$
						$7.030(4)^R$
						$7.024(5)^{Z2}$
						7.028^{K*13}
Ni-6	$3s^2 3p^6 3d^{10}$	$(3s^2 3p^6 3d^3_{3/2} 3d^6_{5/2} 4p_{3/2})_1$	1829.4	1829.6(4)	6.7766(15)	$6.779(3)^M$
						$6.785(5)^R$
						$6.775(5)^{Z2}$
						6.779^{K*14}
Ni-7	$3s^2 3p^6 3d^{10}$	$(3s^2 3p^2_{1/2} 3p^3_{3/2} 3d^{10} 4s_{1/2})_1$	2017.4	2015.4(3)	6.1518(9)	$6.155(4)^R$
						$6.154(5)^{Z2}$
Ni-8	$3s^2 3p^6 3d^{10}$	$(3s^2 3p^6 3d^4_{3/2} 3d^5_{5/2} 4f_{7/2})_1$	2112.6	2112.2(3)	5.8699(8)	5.867^{N*15}
						$5.872(2)^R$
						$5.871(3)^{Z2}$
						$5.8715(8)^B$
Ni-9	$3s^2 3p^6 3d^{10}$	$(3s^2 3p^6 3d^3_{3/2} 3d^6_{5/2} 4f_{5/2})_1$	2181.4	2179.7(4)	5.6881(10)	5.690^{N*16}
						$5.691(2)^R$
						$5.689(3)^{Z2}$
						$5.6913(8)^B$
Ni-10	$3s^2 3p^6 3d^{10}$	$(3s^2 3p_{1/2} 3p^4_{3/2} 3d^{10} 4s_{1/2})_1$	2323.6	2320.3(6)	5.3435(14)	
Ni-11	$3s^2 3p^6 3d^{10}$	$(3s^2 3p^2_{1/2} 3p^3_{3/2} 3d^{10} 4d_{3/2})_1$	2361.8	2360.7(7)	5.2520(16)	5.2509^{N*17}
						$5.255(2)^T$
Ni-12	$3s^2 3p^6 3d^{10}$	$(3s^2 3p^2_{1/2} 3p^3_{3/2} 3d^{10} 4d_{5/2})_1$	2386.0	2384.2(4)	5.2002(9)	5.1963^{N*18}
						$5.203(2)^T$
						$5.203(3)^R$
Ni-13	$3s^2 3p^6 3d^{10}$	$(3s^2 3p^2_{1/2} 3p^3_{3/2} 3d^{10} 4f_{7/2})_2$	2554.7	2553.0(4)	4.8564(8)	$4.857(2)^T$
						4.857^W
Ni-14	$3s^2 3p^6 3d^{10}$	$(3s_{1/2} 3p^6 3d^{10} 4p_{1/2})_1$	2655.0	2651.3(4)	4.6764(7)	$4.680(2)^T$
Ni-15	$3s^2 3p^6 3d^{10}$	$(3s^2 3p_{1/2} 3p^4_{3/2} 3d^{10} 4d_{3/2})_1$	2678.6	2673.7(6)	4.6372(10)	$4.638(2)^T$
Ni-16	$3s^2 3p^6 3d^{10}$	$(3s_{1/2} 3p^6 3d^{10} 4p_{3/2})_1$	2765.6	2760.7(5)	4.4910(8)	$4.493(2)^T$
Ni-17	$3s^2 3p^6 3d^{10}$	$(3s^2 3p^6 3d^4_{3/2} 3d^5_{5/2} 5f_{7/2})_1$	2814.9	2816.1(3)	4.4027(5)	$4.406(2)^T$
						$4.403(2)^R$
						4.409^{Z1*19}
Ni-18	$3s^2 3p^6 3d^{10}$	$(3s^2 3p^6 3d^3_{3/2} 3d^6_{5/2} 5f_{5/2})_1$	2877.3	2878.2(3)	4.3077(4)	$4.309(2)^R$
						$4.309(2)^T$
						4.311^{Z1}
Ni-19	$3s^2 3p^6 3d^{10}$	$(3s^2 3p^2_{1/2} 3p^3_{3/2} 3d^{10} 5d_{5/2})_1$	3183.9	3182.7(4)	3.8956(5)	$3.895(2)^T$
Ni-20	$3s^2 3p^6 3d^{10}$	$(3s^2 3p^6 3d^4_{3/2} 3d^5_{5/2} 6f_{7/2})_1$	3195.5	3196.8(3)	3.8784(4)	$3.877(2)^T$
						$3.878(2)^R$
						3.879^{Z1}
Ni-21	$3s^2 3p^6 3d^{10}$	$(3s^2 3p^6 3d^3_{3/2} 3d^6_{5/2} 6f_{5/2})_1$	3258.9	3259.9(3)	3.8033(4)	$3.803(2)^T$
						$3.800(2)^R$
						3.803^{Z1}
Ni-22	$3s^2 3p^6 3d^{10}$	$(3s^2 3p^6 3d^4_{3/2} 3d^5_{5/2} 7f_{7/2})_1$	3424.4	3426.0(4)	3.6189(4)	$3.618(2)^T$
Ni-23	$3s^2 3p^6 3d^{10}$	$(3s^2 3p_{1/2} 3p^4_{3/2} 3d^{10} 5d_{3/2})_1$	3482.7	3480.9(7)	3.5618(7)	$3.551(2)^T$
Ni-24	$3s^2 3p^6 3d^{10}$	$(3s^2 3p^6 3d^3_{3/2} 3d^6_{5/2} 7f_{5/2})_1$	3488.9	3490.2(4)	3.5524(4)	$3.551(2)^T$
Ni-25	$3s^2 3p^6 3d^{10}$	$(3s^2 3p^6 3d^4_{3/2} 3d^5_{5/2} 8f_{7/2})_1$	3572.5	3574.1(5)	3.4690(5)	$3.469(2)^T$
Ni-26	$3s^2 3p^6 3d^{10}$	$(3s^2 3p^2_{1/2} 3p^3_{3/2} 3d^{10} 6d_{5/2})_1$	3600.9	3600.0(6)	3.4440(6)	$3.445(2)^{T*20}$
Ni-27	$3s^2 3p^6 3d^{10}$	$(3s^2 3p^6 3d^3_{3/2} 3d^6_{5/2} 8f_{5/2})_1$	3637.7	3639.5(6)	3.4066(6)	

Table 4. Ni-like W^{46+} line positions measured with the NASA XRS spectrometer. Theoretical energies are from the present FAC calculations. ^{B} Butzbach et al. [42], ^{K} Klapisch et al. [22], ^{M} Mandelbaum et al. [23], ^{N} Neill et al. [12], ^{Ne} Neu et al. [13], ^{R} Ralchenko et al. [19], ^{T} Tragin et al. [24], ^{W} Wyart et al. [43], ^{Z1} Zigler et al. [11], ^{Z2} Zigler et al. [10]. Superscripts *xx denote comments on previous measurement found in Table 6.

Key	Transition lower level	upper level	Theory ΔE (eV)	Experiment ΔE (eV)	λ (Å)	Prev. Exp. λ (Å)
Co-1	$3s^23p^63d^4_{3/2}3d^5_{5/2}$	$(3s^23p^63d^4_{3/2}3d^4_{5/2}4s_{1/2})_{9/2}$	1607.3	1607.6(4)	7.7124(19)	
		$(3s^23p^63d^4_{3/2}3d^4_{5/2}4s_{1/2})_{7/2}$	1610.5			
Co-2	$3s^23p^63d^4_{3/2}3d^5_{5/2}$	$(3s^23p^63d^4_{3/2}3d^4_{5/2}4s_{1/2})_{5/2}$	1617.0	1617.2(10)	7.6666(47)	
		$(3s^23p^63d^4_{3/2}3d^4_{5/2}4s_{1/2})_{3/2}$	1618.4			
	$3s^23p^2_{1/2}3p^3_{3/2}3d^{10}$	$(3s^23p^63d^3_{3/2}3d^5_{5/2}4d_{3/2})_{5/2}$	1621.4			
	$3s^23p^63d^3_{3/2}3d^6_{5/2}$	$(3s^23p^63d^3_{3/2}3d^5_{5/2}4s_{1/2})_{7/2}$	1622.4			
Co-3	$3s^23p^63d^4_{3/2}3d^5_{5/2}$	$(3s^23p^63d^3_{3/2}3d^5_{5/2}4s_{1/2})_{9/2}$	1688.3	1686.8(5)	7.3503(22)	
Co-4	$3s^23p^63d^4_{3/2}3d^5_{5/2}$	$(3s^23p^63d^3_{3/2}3d^5_{5/2}4p_{1/2})_{7/2}$	1785.4	1783.8(8)	6.9506(31)	$6.949(3)^M$ 6.949^K
		$(3s^23p^63d^3_{3/2}3d^5_{5/2}4p_{1/2})_{3/2}$	1785.5			$6.949(3)^M$ 6.949^K
Co-5	$3s^23p^63d^4_{3/2}3d^5_{5/2}$	$(3s^23p^63d^4_{3/2}3d^4_{5/2}4p_{3/2})_{7/2}$	1812.6	1812.4(8)	6.8409(30)	$6.844(3)^M$ 6.844^K
		$(3s^23p^63d^4_{3/2}3d^4_{5/2}4p_{3/2})_{5/2}$	1813.0			$6.844(3)^M$ 6.844^K
Co-6	$3s^23p^63d^4_{3/2}3d^5_{5/2}$	$(3s^23p^63d^4_{3/2}3d^4_{5/2}4p_{3/2})_{5/2}$	1818.9	1820.6(8)	6.8101(30)	
		$(3s^23p^63d^4_{3/2}3d^4_{5/2}4p_{3/2})_{3/2}$	1822.8			$6.806(3)^{M*21}$ 6.806^K
Co-7	$3s^23p^63d^4_{3/2}3d^5_{5/2}$	$(3s^23p^2_{1/2}3p^3_{3/2}3d^4_{3/2}3d^5_{5/2}4s_{1/2})_{7/2}$	2063.2	2062.4(10)	6.0116(29)	
		$(3s^23p^2_{1/2}3p^3_{3/2}3d^4_{3/2}3d^5_{5/2}4s_{1/2})_{5/2}$	2066.8			
Co-8	$3s^23p^63d^4_{3/2}3d^5_{5/2}$	$(3s^23p^2_{1/2}3p^3_{3/2}3d^4_{3/2}3d^5_{5/2}4s_{1/2})_{3/2}$	2075.1	2072.9(10)	5.9812(29)	
Co-9	$3s^23p^63d^4_{3/2}3d^5_{5/2}$	$(3s^23p^63d^4_{3/2}3d^4_{5/2}4f_{5/2})_{5/2}$	2133.5	2137.1(10)	5.8015(27)	
		$(3s^23p^63d^4_{3/2}3d^4_{5/2}4f_{5/2})_{7/2}$	2136.0			
	$3s^23p^2_{1/2}3p^3_{3/2}3d^{10}$	$3s^23p^2_{1/2}3p^3_{3/2}3d^4_{3/2}3d^5_{5/2}4f_{5/2})_{1/2}$	2136.3			
		$3s^23p^2_{1/2}3p^3_{3/2}3d^4_{3/2}3d^5_{5/2}4f_{5/2})_{5/2}$	2137.6			
	$3s^23p^63d^4_{3/2}3d^5_{5/2}$	$(3s^23p^63d^4_{3/2}3d^4_{5/2}4f_{5/2})_{3/2}$	2138.0			
	$3s^23p^2_{1/2}3p^3_{3/2}3d^{10}$	$3s^23p^2_{1/2}3p^3_{3/2}3d^4_{3/2}3d^5_{5/2}4f_{5/2})_{3/2}$	2138.5			
	$3s^23p^63d^4_{3/2}3d^5_{5/2}$	$(3s^23p^63d^4_{3/2}3d^4_{5/2}4f_{7/2})_{7/2}$	2140.1			
Co-10	$3s^23p^63d^4_{3/2}3d^5_{5/2}$	$(3s^23p^63d^4_{3/2}3d^4_{5/2}4f_{7/2})_{5/2}$	2145.9	2146.9(10)	5.7750(27)	
		$(3s^23p^63d^4_{3/2}3d^4_{5/2}4f_{7/2})_{3/2}$	2147.7			5.7744^{N*22}
Co-11	$3s^23p^63d^4_{3/2}3d^5_{5/2}$	$(3s^23p^63d^4_{3/2}3d^4_{5/2}4f_{7/2})_{5/2}$	2155.9	2156.8(4)	5.7485(11)	5.7531^{N*23}
		$(3s^23p^63d^4_{3/2}3d^4_{5/2}4f_{7/2})_{7/2}$	2157.9			5.7482^{N*23}
		$(3s^23p^63d^4_{3/2}3d^4_{5/2}4f_{5/2})_{5/2}$	2160.4			
	$3s^23p^63d^3_{3/2}3d^6_{5/2}$	$(3s^23p^63d^3_{3/2}3d^5_{5/2}4f_{7/2})_{5/2}$	2160.8			
Co-12	$3s^23p^63d^4_{3/2}3d^5_{5/2}$	$(3s^23p^63d^3_{3/2}3d^5_{5/2}4f_{5/2})_{3/2}$	2223.8	2227.1(4)	5.5671(10)	5.5811^{N*24}
		$(3s^23p^63d^3_{3/2}3d^5_{5/2}4f_{7/2})_{5/2}$	2227.4			5.5713^{N*25}
		$(3s^23p^63d^3_{3/2}3d^5_{5/2}4f_{5/2})_{7/2}$	2229.9			5.5686^{N*26}
		$(3s^23p^63d^3_{3/2}3d^5_{5/2}4f_{5/2})_{5/2}$	2230.9			5.5641^{N*27}
Co-13	$3s^23p^63d^4_{3/2}3d^5_{5/2}$	$(3s^23p^63d^4_{3/2}3d^4_{5/2}5f_{7/2})_{5/2}$	2889.4	2890.3(5)	4.2897(7)	$4.289(2)^{T*28}$
		$(3s^23p^63d^4_{3/2}3d^4_{5/2}5f_{7/2})_{7/2}$	2891.0			$4.289(2)^{T*28}$
Co-14	$3s^23p^63d^4_{3/2}3d^5_{5/2}$	$(3s^23p^63d^3_{3/2}3d^5_{5/2}5f_{5/2})_{3/2}$	2956.4	2957.9(4)	4.1916(6)	$4.192(2)^{T*29}$
		$(3s^23p^63d^3_{3/2}3d^5_{5/2}5f_{5/2})_{7/2}$	2957.7			$4.192(2)^{T*29}$
		$(3s^23p^63d^3_{3/2}3d^5_{5/2}5f_{5/2})_{5/2}$	2957.9			$4.192(2)^{T*29}$

Table 5. Co-like W^{47+} line positions measured with the NASA XRS spectrometer. Theoretical energies are from the present FAC calculations. ^{K} Klapisch et al. [22], ^{M} Mandelbaum et al. [23], ^{N} Neill et al. [12], ^{T} Tragin et al. [24]. Superscripts *xx denote comments on previous measurement found in Table 6.

Key	Reference	Comment
$*^{1}$	Mandelbaum et al. [23]	Average λ of a broad feature. PW assigned several transitions to feature.
$*^{2}$	Neill et al. [12]	Average λ from five line lists. PW assigned the line to Ga-like W.
$*^{3}$	Neill et al. [12]	Average λ from three line lists. PW has different assignment.
$*^{4}$	Neill et al. [12]	Average λ from four line lists.
$*^{5}$	Tragin et al. [24] Zigler et al. [11]	PW assigned feature blended with Ge-like W line.
$*^{6}$	Mandelbaum et al. [23]	PW assigned several transitions to feature.
$*^{7}$	Mandelbaum et al. [23]	PW assigned two transitions to feature.
$*^{8}$	Neill et al. [12]	Average λ from seven line lists.
$*^{9}$	Neill et al. [12]	Average λ from three line lists.
$*^{10}$	Neill et al. [12]	Average λ from seven line lists.
$*^{11}$	Tragin et al. [24] Zigler et al. [11]	PW assigned feature blended with Ga-like W line.
$*^{12}$	Tragin et al. [24]	PW assigned two transitions to feature.
$*^{13}$	Klapisch et al. [22]	PW has no line assignment.
$*^{14}$	Klapisch et al. [22]	PW has no line assignment.
$*^{15}$	Neill et al. [12]	Average λ from ten line lists.
$*^{16}$	Neill et al. [12]	Average λ from ten line lists.
$*^{17}$	Neill et al. [12]	Average λ from five line lists.
$*^{18}$	Neill et al. [12]	Average λ from ten line lists.
$*^{19}$	Zigler et al. [11]	PW assigned two transitions to feature.
$*^{20}$	Tragin et al. [24]	PW assigned two transitions to feature.
$*^{21}$	Mandelbaum et al. [23]	PW assigned two transitions to feature.
$*^{22}$	Neill et al. [12]	Average λ from five line lists.
$*^{23}$	Neill et al. [12]	Average λ from five line lists.
$*^{24}$	Neill et al. [12]	Average λ from seven line lists.
$*^{25}$	Neill et al. [12]	Average λ from five line lists. PW has different assignment.
$*^{26}$	Neill et al. [12]	Average λ from eight line lists.
$*^{27}$	Neill et al. [12]	Average λ from six line lists.
$*^{28}$	Tragin et al. [24]	PW has no line assignment.
$*^{29}$	Tragin et al. [24]	PW has no line assignment.

Table 6. Comments on the selection of the lines from previous work (PW) and earlier line assignments.